IEEE Access
Multidisciplinary | Rapid Review | Open Access Journal

Received December 12, 2018, accepted December 17, 2018, date of publication January 18, 2019, date of current version February 8, 2019.

Digital Object Identifier 10.1109/ACCESS.2019.2892714

Performance Analysis of Improved Energy Detector With Hardware Impairments for Accurate Spectrum Sensing

LEILA TLEBALDIYEVA[1], THEODOROS A. TSIFTSIS[2], (Senior Member, IEEE), AND BEHROUZ MAHAM[1], (Senior Member, IEEE)

[1]Department of Electrical and Computer Engineering, Nazarbayev University, Astana Z05H0P9, Kazakhstan
[2]School of Electrical and Computer Engineering, Jinan University, Zhuhai 519070, China

Corresponding author: Leila Tlebaldiyeva (ltlebaldiyeva@nu.edu.kz)

This work was supported by Nazarbayev University.

ABSTRACT The impact of transceiver hardware impairments on the accuracy of spectrum sensing cannot be ignored in low-cost and high data rate cognitive radio systems. Nevertheless, ideal hardware for spectrum sensing is widely assumed in the technical literature. This paper presents a novel method for evaluating the improved energy detector (IED) statistics using α-μ distribution over additive white Gaussian noise (AWGN) and Nakagami-m fading channel by considering transceiver hardware imperfections. Moreover, the performance of the IED over AWGN channel is highlighted by the area under the receiver operating curve. Furthermore, the average probability of detection is evaluated for both fading and non-fading environments. An asymptotic analysis studies detection probability over fading channels at a low average signal-to-noise-ratio region. Moreover, p-order law combining and p-order law selecting diversity techniques are proposed to increase the performance of the detector. Our simulation results demonstrate that the diversity techniques significantly improve the detector performance.

INDEX TERMS Area under the ROC curve (AUC), α-μ distribution, false alarm probability, improved energy detector, Nakagami-m fading channel, probability of detection, receiver operating characteristic (ROC) curve, transceiver hardware impairments.

I. INTRODUCTION

Improved energy detector (IED) is a type of non-coherent energy detector that can detect the presence of a primary user signal in cognitive radio (CR) systems. The IED is an advanced version of conventional energy detector (ED), which is a square law device that evaluates energy of the primary user (PU) signal over a period of time [1]. The IED raises an amplitude of each signal sample to the arbitrary positive power p and adds up to yield a test statistics as originally presented by Chen [2]. Similar to the conventional ED, the IED does not require channel state information (CSI) and provides a quick-sensing decision.

A. TECHNICAL LITERATURE REVIEW

The IED demonstrated enhanced performance in comparison with the conventional ED [2]–[4]. Gamma function approximations were used to derive a distribution of the IED test statistics by matching the values of the mean and variance for the H_0 and H_1 test statistics in Gaussian noise [2]. Gahane *et al.* [4] have applied the IED to mobile cognitive users in cooperative cognitive networks over generalized Nakagami-m, Nakagami-q, $\kappa - \mu$, and $\nu - \mu$ fading channels, where the receiver operating characteristic (ROC) curves and area under the ROC curves (AUC) were studied.

The performance of cooperative spectrum sensing in multihop CR network using multiple antennas was implemented using the IED in [3]. Numerical results of this work have stated that the IED significantly outperformed the conventional ED. One of the recent works on the IED over Rayleigh, Hoyt, and Rician fading channels studied a censoring-based cooperative spectrum sensing in [5]. The authors concluded that the censoring threshold of a secondary user (SU) has a great influence on the average miss detection probability. In addition, it was proven that the system performance improved when the number of SUs, antennas, and signal-to-noise-ratio (SNR) values for reporting and sensing channels were increased. Nevertheless, the main drawback of cooperative spectrum sensing is a requirement of a large number of SU devices, which results in latency for decision-making [6].

Gahane and Sharma [7] investigated the performance of the IED for cooperative CR with selection combining diversity. Moreover, cognitive user mobility and imperfect channel state information were considered while evaluating probability of miss detection, probability of false alarm, and error performance over Rayleigh fading channel. However, detection statistics in [7] were derived based on one sample of the signal. Antenna selection diversity was studied in [8] for cooperative spectrum sensing network over additive white Gaussian noise (AWGN) and Rayleigh environments, where detection statistics was also based on one signal sample as in the previous work. Moreover, optimization analysis was performed for an optimum number of normalized SUs and threshold values.

Blind and robust spectrum sensing was enabled in [9] by suggesting mitigation and sensing functions that minimize negative impacts of hardware impairment noises. Mitigation algorithm filtered out undesired frequency components originating from radio frequency (RF) non-linearity. Practical implementation of the proposed two-stage algorithm consisting of two software defined radio blocks, USRPs and N210, was built to record real measurements. Experimental results validated theoretical results and showed an improvement in the probability of false alarm performance.

Boulogeorgos *et al.* [10] studied spectrum sensing using conventional ED under RF hardware impairments. Hardware impairment noises originated from direct-conversion radio (DCR) receivers such as in-phase (I) and quadrature-phase (Q) imbalance (I/Q imbalance), low-noise amplifier nonlinearities, and phase noise were modeled and studied for the multichannel environment in [10]. It was shown that RF impairments have a detrimental effect on spectrum sensing. In addition, the effect of I/Q imbalance was studied for the conventional ED in [11], and four level hypotheses test was proposed for conventional ED performance. In addition, Imana *et al.* [12] investigated receiver I/Q imbalance and aliasing on multi-band spectrum sensing, and proposed a new spectrum mechanism they refer to as robust swept-multi-band spectrum sensing (RS-MSS). This proposed new spectrum sensing mechanism aimed to increase the accuracy of the signal detection. The RS-MSS eliminated the effects of distortion noises originating from I/Q imbalance and aliasing and used channelized spectrum representation (CSR) to model the receiver. The proposed solution has been tested by simulations and verified by hardware experiments and showed a higher performance in comparison to conventional EDs. In addition, Mehrabian and Zaimbashi [13] have modeled a single-input-multiple-output (SIMO) cognitive radio receiver distorted by I/Q imbalance of the transmitter. Eigenvalue-based detectors called Wald and Rao were introduced and their detection performance was compared by Monte Carlo simulations. DCR are widely used for low-cost CR receivers, however, oscillator phase noise in DRC causes crosstalk between simultaneously transmitting channels. Gokceoglu *et al.* [14], [15] analyzed oscillator phase noise and I/Q imbalance in multichannel direct-conversion receivers. An enhanced energy detection technique was proposed to mitigate I/Q imbalance and phase noise. This technique increased spectrum sensing accuracy in the presence of oscillator phase noise and I/Q imbalance. Spectrum sensing in a full-duplex CR under I/Q imbalance was studied in [16] for single and multichannel conventional ED. Moreover, transceiver hardware impairments studied in [17]–[22] investigated the effect of electronic imperfections on the wireless communication system performance.

B. MOTIVATION

Our work is motivated by the importance of modeling hardware impairment noises for accurate spectrum sensing. To the best of the authors' knowledge, hardware impairments for the IED have not yet been studied, and it could be a significant tool for the development of reliable receivers. Therefore, we study the effect of joint hardware impairments on the spectrum sensing performance using the IED, and propose p-order law combining (pLC) and p-order law selecting (pLS) diversity techniques to overcome adverse effects of transceiver impairments.

C. OUR CONTRIBUTIONS

The contributions of this work are outlined below:

- A new approach for evaluating test statistics for the IED is presented using the $\alpha - \mu$ approximation for a signal sample size equal to N for ideal and non-ideal system configurations.
- The AUC analysis is performed for both ideal and non-ideal system models over AWGN channel.
- Analytical closed-form expressions for the average detection probability over Nakagami-m channels are derived for ideal and non-ideal IED.
- We present closed-form expressions for the probability of detection of the pLC and the pLS diversity techniques over AWGN channel. Moreover, the average detection probabilities over Rayleigh/Nakagami-m fading channels are presented for diversity receivers under ideal and non-ideal hardware models.
- Asymptotic results are derived for low SNR values.
- Numerical results demonstrate that hardware impairment noises degrade system performance and reveal that the pLC and the pLS diversity techniques contribute to overcome negative effects of hardware imperfections.
- Total error rate analysis is performed to test the IED performance while implementing non-diversity and diversity receivers by considering both ideal and non-ideal system configurations.

The structure of this paper is organized as follows. Section II presents the System and Signal model for ideal and hardware impaired system configurations. Section III describes the derivation of the IED using $\alpha - \mu$ distribution, followed by Section IV, wherein the detection and false alarm probabilities over AWGN channel for both ideal and non-ideal hardware-impaired cases are derived. In Section V,

the average detection and the false alarm probabilities are formulated over Nakagami-*m* fading channels. In Section VI, diversity receivers using the *p*LC and *p*LS techniques are proposed to minimize the effects of hardware impairments. In Section VII, we verify our analytical expressions through numerical simulations. The main concluding statements of this work are summarized in Section VIII.

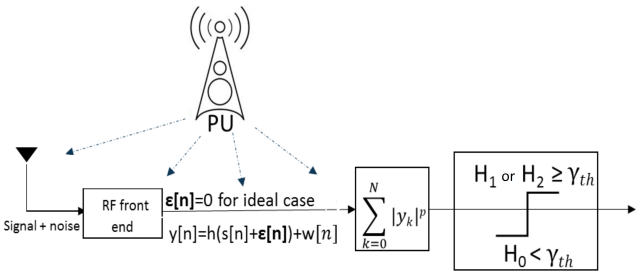

FIGURE 1. System model for improved energy detector for non-diversity SU receiver.

II. SYSTEM AND SIGNAL MODEL

We consider a CR network with one PU and a single antenna SU for a non-diversity signal reception as shown in Fig. 1. The IED is employed at the SU for the detection of possible PU activity. Based on the signal power, a two-level hypotheses test is applied for both ideal and hardware impaired energy detectors for identifying whether the spectrum is occupied by primary transmissions. The absence of the PU signal is given as the hypothesis H_0. On the other hand, the presence of the PU signal in Gaussian noise at ideal hardware is modeled as the hypothesis H_1. In addition, for the system with hardware impairments, the hypothesis H_2 is applied to detect the signal in Gaussian plus hardware distortion noises as follows

$$\begin{aligned} H_0 &: y[n] = w[n] \\ H_1 &: y[n] = hs[n] + w[n] \\ H_2 &: y[n] = h(\varepsilon[n] + s[n]) + w[n], \end{aligned} \tag{1}$$

where $y[n]$ is a received signal, a PU signal $s[n]$ is a complex transmitted signal with average signal power $P = \mathbb{E}\{|s[n]|^2\}$, where $\mathbb{E}\{\cdot\}$ denotes expectation operator. In (1), the wireless channel gain coefficient h is assumed to be either deterministic for AWGN or random for Nakagami-*m* distribution. In addition, $w[n]$ is a circularly symmetric complex Gaussian noise variable with zero mean and σ_w^2 variance $w[n] \sim \mathcal{CN}(0, \sigma_w^2)$, aggregate distortion noises originating from the transmitter and the receiver hardware impairments are represented by $\varepsilon[n]$, where $\varepsilon[n] \sim \mathcal{CN}(0, \kappa^2 P)$. Note that κ indicates the compound hardware impairment level originated from the transmitter and the receiver sides and measured by error vector magnitude (EVM).[1] Moreover, κ varies according to modulation type and protocol requirements, and it is evaluated as $\kappa = \sqrt{\kappa_t^2 + \kappa_r^2}$ [17], where κ_t stands for the transmitter hardware impairment and κ_r for the receiver hardware impairment level. We have adopted the aggregate transceiver hardware impairment model from [23]. This model combines the residual distortion noises from I/Q imbalance, amplifier non-linearity, and oscillator phase noise. This simple yet comprehensive model was theoretically and practically supported by [17] and [23]–[26].

The instantaneous signal-to-noise-distortion ratio (SNDR) of the system with hardware impairments is given in [17] as

$$\gamma_{\text{hi}} = \frac{|h|^2 P}{|h|^2 \kappa^2 P + \sigma_w^2} = \frac{\gamma}{\kappa^2 \gamma + 1}, \tag{2}$$

where γ denotes instantaneous SNR and defined as $\gamma = \frac{P|h|^2}{\sigma_w^2}$.

III. IMPROVED ENERGY DETECTOR

In this section, we introduce an alternative derivation of the IED using the sum of N independent and identically distributed (i.i.d.) Weibull random variables (RVs) that is approximated to $\alpha - \mu$ distribution. The mathematical formulation of the IED for the hypothesis test is given by

$$\Lambda = \sum_{i=1}^{N} Y_i \underset{H_0}{\overset{H_1, H_2}{\gtrless}} \gamma_{th}, \tag{3}$$

and

$$Y_i = \left(\frac{|y_i|}{\sigma_w}\right)^p, \tag{4}$$

where Λ is the test statistics to considered hypothesis test, Y_i is a RV that represents one sample of the IED normalized to the noise power, γ_{th} is a detection threshold, N denotes the number of signal samples, and p is a positive power level. Inspired by [3, eqs. (7) and (8)], the conditional probability density functions (PDFs) of the Y_i under H_0 and H_1 hypotheses are represented by $f_{Y_i|H_0}(x)$ and $f_{Y_i|H_1}(x)$, respectively, and given as

$$f_{Y_i|H_0}(x) = \frac{2x^{\frac{2-p}{p}} \exp(-x^{\frac{2}{p}})}{p}, \tag{5}$$

$$f_{Y_i|H_1}(x) = \frac{2x^{\frac{2-p}{p}} \exp(-\frac{x^{\frac{2}{p}}}{1+\gamma})}{p(1+\gamma)}. \tag{6}$$

By extending this analysis, the PDF of the Y_i for hardware-impaired system model can be introduced as

$$f_{Y_i|H_2}(x) = \frac{2x^{\frac{2-p}{p}} \exp(-\frac{x^{\frac{2}{p}}}{1+\gamma_{\text{hi}}})}{p(1+\gamma_{\text{hi}})}. \tag{7}$$

The PDF of Y_i RVs for the hypothesis shown above in (5-7) follows the Weibull distribution given as [27]

$$f(x|a,b,c) = \frac{c}{b}\left(\frac{x-a}{b}\right)^{(c-1)} \exp\left\{-\left(\frac{x-a}{b}\right)^c\right\}, \tag{8}$$

[1] EVM is a measure of the transceiver performance quality which is influenced by I/Q phase shift, amplifier non-linearity, AWGN, and phase noise [23]. EVM is a Figure of Merit that evaluates transceiver performance measured in dB or percentage.

where $x \geq a; a \in \mathbb{R}; b, c \in \mathbb{R}^+$ and $\mathbb{R}$ stands for real numbers. According to (3), the IED is a sum of N Weibull distributed RVs. Simple and precise approximations to N Weibull sums are modeled by the $\alpha - \mu$ distribution as presented in [28]. The PDF and the cumulative distribution function (CDF) of $\alpha - \mu$ distribution are shown as [29]

$$f_\Lambda(x) = \frac{\alpha \mu x^{\alpha\mu-1}}{\Omega^\mu \Gamma(\mu)} \exp(-\frac{\mu x^\alpha}{\Omega}), \tag{9}$$

$$F_\Lambda(x) = 1 - \frac{\Gamma(\mu, \frac{\mu x^\alpha}{\Omega})}{\Gamma(\mu)}, \tag{10}$$

respectively, where $\alpha > 0$ is a shape parameter, $\mu = \mathbb{E}^2[\Lambda^\alpha]/\sigma_{\Lambda^\alpha}$ is an inverse of the normalized variance, $\Omega = \mathbb{E}[\Lambda^\lambda]$ is a scale parameter, $\Gamma(\cdot,\cdot)$ is an incomplete Gamma function [30, eq. (8.350.2)] and $\Gamma(\cdot)$ [30, eq. (8.310.1)] denotes Gamma function. In order to evaluate α, μ, and Ω parameters, moment-based estimators of these parameters and exact moment-based estimators of Λ are calculated, and the system of equations is numerically solved for α and μ parameters as in [28]

$$\frac{\Gamma^2(\mu+\frac{1}{\alpha})}{\Gamma(\mu)\Gamma(\mu+\frac{2}{\alpha}) - \Gamma^2(\mu+\frac{1}{\alpha})} = \frac{\mathbb{E}^2[\Lambda]}{\mathbb{E}[\Lambda^2] - \mathbb{E}^2[\Lambda]}, \tag{11}$$

$$\frac{\Gamma^2(\mu+\frac{2}{\alpha})}{\Gamma(\mu)\Gamma(\mu+\frac{4}{\alpha}) - \Gamma^2(\mu+\frac{1}{\alpha})} = \frac{\mathbb{E}^2[\Lambda^2]}{\mathbb{E}[\Lambda^4] - \mathbb{E}^2[\Lambda^2]}, \tag{12}$$

where the first, second, and fourth order moments of the IED test statistics, namely $\mathbb{E}[\Lambda]$, $\mathbb{E}[\Lambda^2]$, and $\mathbb{E}[\Lambda^4]$ are calculated by using following set of equations given as

$$\mathbb{E}[\Lambda^n] = \sum_{n_1=0}^{n} \sum_{n_2=0}^{n_1} \cdots \sum_{n_{N-1}=0}^{n_{N-2}} \binom{n}{n_1}\binom{n_1}{n_2}\cdots\binom{n_{N-2}}{n_{N-1}} \times \mathbb{E}[\Lambda_1^{n-n_1}]\mathbb{E}[\Lambda_2^{n_1-n_2}]\cdots\mathbb{E}[\Lambda_N^{n_{N-1}}], \tag{13}$$

where n is the order of the moment; $\mathbb{E}[\Lambda_i^n]$ can be calculated as

$$\mathbb{E}[\Lambda_i^n] = \Phi^{\frac{n}{\beta}} \Gamma\left(1 + \frac{n}{\beta}\right), \tag{14}$$

where $\beta = 2/p$, and $\Phi = 1$ for H_0 hypothesis, $\Phi = 1+\gamma$ for H_1 hypothesis, and, finally, $\Phi = 1 + \gamma_{\text{hi}}$ for H_2 hypothesis. We present a detailed derivation of the Λ moments in Appendix A and summarize their closed-form expressions as

$$\mathbb{E}[\Lambda] = N\Phi^{\frac{1}{\beta}}\Gamma\left(\frac{1}{\beta}+1\right), \tag{15}$$

$$\mathbb{E}[\Lambda^2] = (N-1)N\Phi^{\frac{2}{\beta}}\left(\Gamma(\frac{1}{\beta}+1)\right)^2 + N\Phi^{\frac{2}{\beta}}\Gamma\left(\frac{2}{\beta}+1\right), \tag{16}$$

$$\mathbb{E}[\Lambda^4] = N\Phi^{\frac{4}{\beta}}\Big(\Gamma(\frac{4}{\beta}+1) + (N-3)(N-2)(N-1)N \times \left(\Gamma(\frac{1}{\beta}+1)\right)^4 + 6(N-2)(N-1)\Gamma(\frac{2}{\beta}+1) \times \left(\Gamma(\frac{1}{\beta}+1)\right)^2 + 4(N-1)\Gamma(\frac{3}{\beta}+1)\Gamma(\frac{1}{\beta}+1) + 3(N-1) \times \left(\Gamma(\frac{2}{\beta}+1)\right)^2\Big). \tag{17}$$

Further, we describe the Ω parameter given in (10). By using [28], we define Ω as a function of α and μ as follows

$$\Omega = \left(\frac{\mu^{\frac{1}{\alpha}}\Gamma(\mu)\Phi^{\frac{1}{\beta}}N\Gamma\left(\frac{1}{\beta}+1\right)}{\Gamma\left(\mu+\frac{1}{\alpha}\right)}\right)^\alpha, \tag{18}$$

where α and μ parameters can be evaluated by (11)-(14).

IV. DETECTION AND FALSE ALARM PROBABILITIES OVER AWGN CHANNELS

In this section, we calculate detection probabilities for ideal and non-ideal hardware, and false alarm probability over AWGN channels. In addition, we present the AUC calculation for AWGN channels. By applying the CDF of $\alpha - \mu$ distribution in (10) and by using the expression for Ω given in (18), we define P_F for the IED over AWGN channels as

$$\begin{aligned} P_F &= \Pr(\Lambda > \gamma_{th}|H_0) \\ &= \frac{1}{\Gamma(\mu_0)}\Gamma\left(\mu_0, \frac{\gamma_{th}^{\alpha_0}}{\left(\frac{\Gamma(\mu_0)N\Gamma(1+\frac{1}{\beta})}{\Gamma(\mu_0+\frac{1}{\alpha_0})}\right)^{\alpha_0}}\right) \\ &= \frac{1}{\Gamma(\mu_0)}\Gamma(\mu_0, \psi_0), \end{aligned} \tag{19}$$

where $\psi_0 = \left(\frac{\gamma_{th}\Gamma\left(\mu_0+\frac{1}{\alpha_0}\right)}{N\Gamma\left(1+\frac{1}{\beta}\right)\Gamma(\mu_0)}\right)^{\alpha_0}$, α_0, and μ_0 parameters are evaluated using equations given in (11)-(12) by setting $\Phi = 1$.

A. P_D^{id} FOR IDEAL SYSTEM MODEL

Analogous to the false alarm probability derivation in (19), we define P_D^{id} as the detection probability for ideal system model over AWGN channel by using (10) and (18) as

$$\begin{aligned} P_D^{\text{id}} &= \Pr(\Lambda > \gamma_{th}|H_1) = \frac{\Gamma\left(\mu_1, \frac{\mu_1\gamma_{th}^{\alpha_1}}{\Omega}\right)}{\Gamma(\mu_1)} \\ &= \frac{1}{\Gamma(\mu_1)}\Gamma\left(\mu_1, \frac{\gamma_{th}^{\alpha_1}}{(\gamma+1)^{\frac{\alpha_1}{\beta}}\left(\frac{\Gamma(\mu_1)N\Gamma(1+\frac{1}{\beta})}{\Gamma(\mu_1+\frac{1}{\alpha_1})}\right)^{\alpha_1}}\right) \\ &= \frac{1}{\Gamma(\mu_1)}\Gamma\left(\mu_1, \frac{\psi_1}{(1+\gamma)^{\frac{\alpha_1}{\beta}}}\right), \end{aligned} \tag{20}$$

where $\psi_1 = \left(\frac{\gamma_{th}\Gamma\left(\mu_1+\frac{1}{\alpha_1}\right)}{N\Gamma\left(1+\frac{1}{\beta}\right)\Gamma(\mu_1)}\right)^{\alpha_1}$ is assigned for a simple representation of the P_D^{id}. Parameters α_1 and μ_1 are evaluated using (11) and (12) by setting $\Phi = 1+\gamma$.

B. P_D^{hi} FOR HARDWARE-IMPAIRED SYSTEM MODEL

In this subsection, we calculate the detection probability of the hardware-impaired system model, P_D^{hi}, over AWGN channels. Hence, we need to modify the moment calculating equation of Λ test statistics in order to incorporate hardware impairment noises. Hence, Weibull moments given in (14) are modified by replacing γ to γ_{hi} as

$$\mathbb{E}[\Lambda_i^n] = \left(\frac{\gamma}{\gamma\kappa^2+1}+1\right)^{\frac{n}{\beta}} \Gamma\left(1+\frac{n}{\beta}\right). \tag{21}$$

Therefore, by using (10) and (21), we calculate P_D^{hi} for the IED under hardware impairments as follows

$$\begin{aligned} P_D^{\text{hi}} &= \Pr(\Lambda > \gamma_{th}|H_2) = \frac{\Gamma\left(\mu_1, \frac{\mu_1\gamma_{th}^{\alpha_1}}{\Omega}\right)}{\Gamma(\mu_1)} \\ &= \frac{1}{\Gamma(\mu_1)}\Gamma\left(\mu_1, \frac{\gamma_{th}^{\alpha_1}}{(\frac{\gamma}{\gamma\kappa^2+1}+1)^{\frac{\alpha_1}{\beta}}\left(\frac{\Gamma(\mu_1)N\Gamma(1+\frac{1}{\beta})}{\Gamma(\mu_1+\frac{1}{\alpha_1})}\right)^{\alpha_1}}\right) \\ &= \frac{1}{\Gamma(\mu_1)}\Gamma\left(\mu_1, \frac{\psi_1}{(\frac{\gamma}{\gamma\kappa^2+1}+1)^{\frac{\alpha_1}{\beta}}}\right), \end{aligned} \tag{22}$$

where α_1, μ_1, and ψ_1 parameters are the same as defined in the previous Section *IV*.*A*.

C. AUC FOR AWGN CHANNEL

The AUC is a single figure of merit that represents a valuable performance metric for evaluating the effectiveness of the detector [31]. AUC values range from 1/2 to 1, where the detector with a better performance approaches to 1. The AUC is a function of the instantaneous SNR value, γ. By using [31] we evaluate the AUC for AWGN channel as

$$A(\gamma) = \int_0^1 P_D(\gamma, \gamma_{th}) dP_F(\gamma_{th}). \tag{23}$$

By using (19) and (20),

$$\begin{aligned} A(\gamma) = \frac{\Gamma(\mu_1+\mu_0)}{\Gamma(\mu_1)\Gamma(\mu_0)} &\frac{\psi_0^{\mu_0}\left(\frac{\eta}{(\gamma+1)^{\frac{\alpha_1}{\beta}}}\right)^{\mu_1}}{\mu_0\left(\frac{\eta}{(\gamma+1)^{\frac{\alpha_1}{\beta}}}+\psi_0\right)^{\mu_1+\mu_0}} \\ &\times {}_2F_1\left(1; \mu_0+\mu_1; \mu_0+1; \frac{\psi_0}{\psi_0+\frac{\eta}{(\gamma+1)^{\frac{\alpha_1}{\beta}}}}\right) \end{aligned} \tag{24}$$

where ${}_2F_1(;;;)$ is the Gauss hypergeometric function [30], $\eta = \left(\frac{\Gamma(\mu_1+1)}{\Gamma(\mu_1 N\Gamma(\frac{1}{\beta}\beta+1)}\right)^{\alpha_1}$, $\mu_0 > 0$, and $(\mu_0+\mu_1) > 0$. In order to calculate the AUC for non-ideal system model, we replace γ by γ_{hi} in (24) as $A(\gamma_{\text{hi}})$. The average AUC for AWGN channel is calculated by replacing instantaneous SNR, γ, by average SNR $\bar{\gamma}$. A full derivation of the AUC over AWGN channel is given in Appendix B.

V. AVERAGE DETECTION PROBABILITIES OVER NAKAGAMI-*m* FADING CHANNELS

This section is devoted to present mathematical calculations for the average detection probabilities over Nakagami-*m* fading channel for ideal and non-ideal system models given as $\bar{P}_{D\text{Nak}}^{\text{id}}$ and $\bar{P}_{D\text{Nak}}^{\text{hi}}$, respectively.

A. $\bar{P}_{\text{DNak}}^{\text{id}}$ FOR IDEAL SYSTEM MODEL

When the signal amplitude follows Nakagami-*m* distribution, the PDF of SNR is represented as

$$f_{\text{Nak}}(\gamma) = \frac{1}{\Gamma(m)}\left(\frac{m}{\bar{\gamma}}\right)^m \gamma^{m-1}\exp\left(-\frac{m}{\bar{\gamma}}\gamma\right), \quad \gamma > 0, \tag{25}$$

where m stands for fading coefficient of the channel. The average detection probability of the IED over Nakagami-*m* fading channels can be evaluated by averaging P_D^{id} in (20) over the PDF of Nakagami-*m* fading channel SNR given in (25). Therefore, $\bar{P}_{D\text{Nak}}^{\text{id}}$ can be evaluated as

$$\begin{aligned} \bar{P}_{D\text{Nak}}^{\text{id}} &= \int_0^\infty P_D^{\text{id}} f_{Nak}(\gamma) d\gamma \\ &= \int_0^\infty \frac{1}{\Gamma(m)}\frac{1}{\Gamma(\mu_1)}(\frac{m}{\bar{\gamma}})^m \gamma^{m-1} e^{-\frac{\gamma m}{\bar{\gamma}}} \\ &\quad \times \Gamma\Big(\mu_1, \frac{\psi_1}{(\gamma+1)^{\frac{\alpha_1}{\beta}}}\Big) d\gamma. \end{aligned} \tag{26}$$

By using series representation of the incomplete Gamma function in [30, eq. (8.354.2)] and some algebraic manipulations, we evaluate the above integral in (26) as

$$\begin{aligned} \bar{P}_{D\text{Nak}}^{\text{id}} = 1 - \epsilon \sum_{n=0}^{\infty}\sum_{j=0}^{\infty} &\frac{(-1)^n(-1)^j}{n!(\mu_1+n)}\psi_1^{\mu_1+n}\binom{s}{j} \\ &\times \sum_{k=0}^{m+j-1}\binom{m+j-1}{k}(-1)^k \Gamma\left(m-k, \frac{m}{\bar{\gamma}}\right), \end{aligned} \tag{27}$$

where ϵ is given as

$$\epsilon = \frac{\left(\frac{m}{\bar{\gamma}}\right)^m}{\Gamma(\mu_1)\Gamma(m)}. \tag{28}$$

A detailed derivation of the $\bar{P}_{D\text{Nak}}^{\text{id}}$ for ideal system model is presented in Appendix *C*.

B. $\bar{P}_{\text{DNak}}^{\text{hi}}$ FOR NON-IDEAL SYSTEM MODEL

In this subsection, we derive average detection probability over Nakagami-*m* fading channel for hardware-impaired system model. Similar to the previous subsection

$$\begin{aligned} \bar{P}_{D\text{Nak}}^{\text{hi}} &= \int_0^\infty P_D^{\text{hi}} f_{Nak}(\gamma) d\gamma \\ &= 1 - \epsilon \sum_{n=0}^{\infty}\sum_{j=0}^{\infty} \frac{(-1)^n (-1)^j \psi_1^{\mu_1+n}}{n!\,(\mu_1+n)}\left(\frac{2}{\beta}(\mu_1+n)j\right) \end{aligned}$$

$$\times \frac{\exp\left(\frac{m}{\bar{\gamma}(1+\kappa^2)}\right)}{(1+\kappa^2)^{m+j}} \sum_{t=0}^{j+m-1} \binom{j+m-1}{t}(-1)^t \times \Gamma\left(m-t, \frac{m}{(1+\kappa^2)\bar{\gamma}}\right)\left(\frac{m}{(1+\kappa^2)\bar{\gamma}}\right)^{t-m}. \quad (29)$$

More derivation steps of the $\bar{P}_{D\text{Nak}}^{\text{hi}}$ are presented in Appendix *D*.

The next section describes asymptotic analysis for the IED over fading channels at low average SNR region.

C. ASYMPTOTIC ANALYSIS AT LOW $\bar{\gamma}$ VALUES

The IED must be able to distinguish a primary user signal from a noise signal. Therefore, it is very crucial to analyze detector's performance at low $\bar{\gamma}$ values. We perform asymptotic analysis of the detector at low $\bar{\gamma}$ values by taking the limit of the $\bar{P}_{D\text{Nak}}^{\text{id}}$ given in (27) when $\bar{\gamma}$ approaches to 0. We expand j summation terms and determine that for $j \neq 0$ all terms are equal to zero and only for $j = 0$ we obtain non-zero term as

$$\lim_{\bar{\gamma}\to 0} \bar{P}_{D\text{Nak}}^{\text{id}} = 1 - \frac{m^m}{\Gamma(\mu_1)} \sum_{n=0}^{\infty} \frac{(-1)^n}{n!(\mu_1+n)} \psi_1^{\mu_1+n}. \quad (30)$$

Asymptotic analysis for $\bar{P}_{D\text{Nak}}^{\text{hi}}$ was not performed due to mathematical complexity of the expression at low $\bar{\gamma}$ values.

VI. DIVERSITY RECEIVERS IN SPECTRUM SENSING

Diversity techniques improve spectrum sensing performance to overcome fading and shadowing effects [32]. Square-law combiner is a square-law device that adds squared signals from M antennas to yield a test statistic [1]. Since the IED uses p-order power of the signal, thus, we propose the p-order Law Combining (pLC) diversity technique. On the other hand, square-law selection technique chooses the highest valued antenna branch to yield a test statistic. Similarly, for the IED case we propose the p-order Law Selection (pLS) diversity technique. In this section, we discuss detection and false alarm probabilities for the diversity receivers using the pLC and the pLS techniques over non-fading and fading channels.

A. DIVERSITY RECEIVERS OVER AWGN CHANNELS

1) pLC

We consider that SU is equipped with M antennas. Diversity receiver's test statistics, D_{pLC}, is an aggregate summation of test statistics from M individual antenna branches. Since one sample of the IED Y_i is Weibull distributed RV, then D_{pLC} is $\alpha - \mu$ distributed RV given as

$$D_{pLC} = \sum_{j=1}^{N}\sum_{i=1}^{M} Y_{ji}. \quad (31)$$

In the pLC technique, we have M times more additions of Weibull distributed RVs. In order to evaluate the probability of false alarm for the pLC technique over i.i.d. AWGN channels, we modify the P_F given in (19) by replacing N to $M \times N$. Hence, we get following result

$$P_{F_c} = \frac{1}{\Gamma(\mu_0)}\Gamma\left(\mu_0, \left(\frac{\gamma_{th}\Gamma(\mu_0+\frac{1}{\alpha_0})}{\Gamma(\mu_0)MN\Gamma(1+\frac{1}{\beta})}\right)^{\alpha_0}\right). \quad (32)$$

Moreover, detection probability for the pLC diversity technique over i.i.d. AWGN channels is calculated by using identical approach used in (32). We substitute N by $M \times N$ in (20) to find detection probability for ideal/non-ideal system by using the pLC technique as

$$P_{D_c}^{\text{id/hi}} = \frac{1}{\Gamma(\mu_1)}\Gamma\left(\mu_1, \left(\frac{\gamma_{th}\Gamma(\mu_1+\frac{1}{\alpha_1})}{(\frac{\gamma}{\kappa^2\gamma+1})^{\frac{\alpha_1}{\beta}}\Gamma(\mu_1)MN\Gamma(1+\frac{1}{\beta})}\right)^{\alpha_1}\right), \quad (33)$$

where $\kappa = 0$ for ideal system model.

2) pLS

Similar to [1], diversity test statistics for the pLS is formed by selecting maximum branch power among M antennas as

$$D_{pLS} = \max(\Lambda_1, \Lambda_2, \cdots, \Lambda_M), \quad (34)$$

where the IED value for antenna i is denoted by Λ_i. Diversity receiver's false alarm and detection probabilities are denoted as P_{F_s} and P_{D_s}, respectively, and evaluated as for conventional ED [1] shown as

$$P_{F_s} = 1 - (1 - P_F)^M, \quad (35)$$

where P_F is defined in (19). Similarly, the detection probability, $P_s^{\text{id/hi}}$, for pLS receiver over AWGN is estimated by

$$P_{D_s}^{\text{id/hi}} = 1 - \prod_{i=1}^{M}(1 - P_{D_i}^{\text{id/hi}}), \quad (36)$$

where $P_{D_i}^{\text{id/hi}}$ is the detection probability for either ideal or hardware impaired system models given in (20) and (22), respectively.

B. DIVERSITY RECEIVERS OVER FADING CHANNELS

1) AVERAGE DETECTION PROBABILITY FOR THE pLC TECHNIQUE

Similar to [1], the average detection probability over i.i.d. Rayleigh fading channels for pLC diversity receiver, $\bar{P}_{D_{c,Ray}}^{\text{id/hi}}$, is equivalent to the average detection probability over Nakagami-m fading channel for non-diversity receivers with $m = M$ and $\bar{\gamma} = M\bar{\gamma}$ substitution given in (26) and (29). Similar approach can be applied to find average detection probability for hardware impaired system model.

2) AVERAGE DETECTION PROBABILITY FOR THE pLS TECHNIQUE

$$\bar{P}_{D_{s,Nak}}^{\text{id/hi}} = 1 - \prod_{i=1}^{M}(1 - \bar{P}_{D_i}^{\text{id/hi}}), \quad (37)$$

where average detection probabilities for ideal/non-ideal system models over Nakagami-m fading channel are given in (27) and (29), respectively.

VII. NUMERICAL EVALUATION

In this section, we demonstrate our simulation results that fully justify analytical derivations presented in Sections IV, V and VI. We demonstrate negative effects of hardware impairment noises for the non-fading and fading channels by using performance analysis metrics such as AUC, ROC, and total error rate. In addition, we investigate the performance gains of the pLC and the pLS techniques for ideal and non-ideal system configurations.

The average detection probability for the ideal system model over fading channels is given in (27), and it is evaluated by using double semi-infinite summations. The detection probability with semi-infinite summation bounds represents exact solution, $\bar{P}_{DNak}^{\text{id, ex}}$ that ranges between $j = [0:\infty)$ and $n = [0:\infty)$, whereas the summation of terms up to a specific positive integer value represents an approximated solution, $\bar{P}_{DNak}^{\text{id, appr}}$ that ranges between $j = [0:a)$ and $n = [0:b)$, where $a > 0$ and $b > 0$.

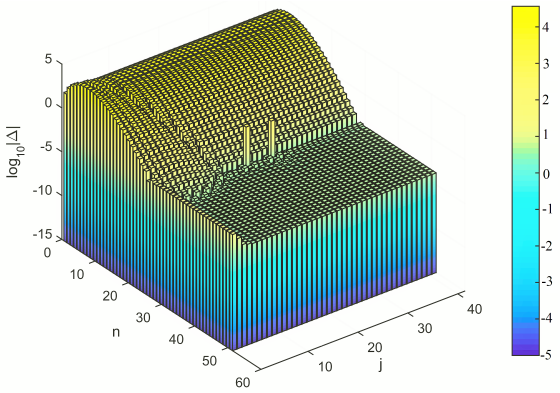

FIGURE 2. Error plot for $\bar{P}_{DNak}^{\text{id,appr}}$ when $j = [0:40]$ and $n = [0:50]$, $m = 2, p = 10, \bar{\gamma} = 0.1$.

In Fig. 2, a logarithmic error plot between exact and approximated detection probabilities is depicted, where $x-axis$ denotes the internal summation size of the $\bar{P}_{DNak}^{\text{id, appr}}$ and ranges between $j = [0:40]$. On the other hand, $y-axis$ denotes the external summation size and ranges between and $n = [0:50]$. An average detection error plot is evaluated by taking arithmetic difference between the exact and the approximated detection probability. Afterwards, this difference is taken as an absolute value and taken as an input to logarithmic function, $\Delta = \log_{10}|\bar{P}_{DNak}^{\text{id,appr}} - \bar{P}_{DNak}^{\text{id, ex}}|$. In Fig. 2, the logarithmic conversion error of the average detection probability is illustrated along $z-axis$. The $\bar{P}_{DNak}^{\text{id,appr}}$ converges relatively fast even at $j = 30$. We can observe from Fig. 2 that internal loop represented by j axes has a significant effect on convergence of the sum rather than external loop denoted by n axis. For instance, at $j = 19$ and $n = 41$ average detection error is as small as $\Delta = 2.29 \times 10^{-4}$,

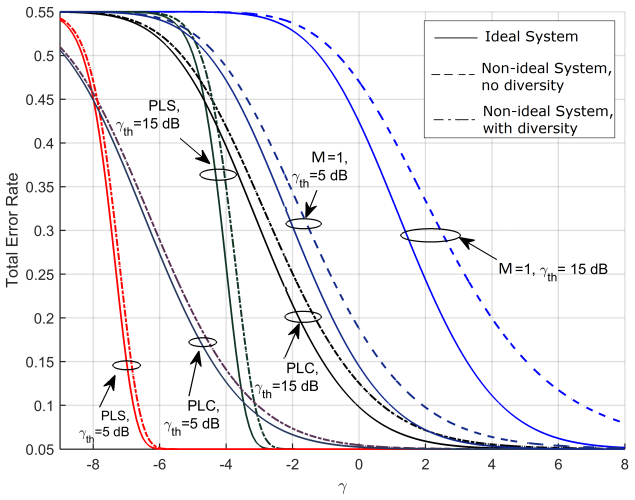

FIGURE 3. Total Error rate for diversity receivers and non-diversity receiver versus SNR over AWGN channels.

which proves fast conversion of the semi-infinite series that represents average detection probability.

In Fig. 3, we present a total error rate versus SNR curves over AWGN channel for non-diversity/diversity receivers when $p = 6$, $N = 5$, number of diversity branches $M = 20$, signal detection threshold $\gamma_{th} = 5$; 15 dB, and $P_F = 0.1$. Note that, total error rate is evaluated as a summation of false alarm and missed detection probabilities [33, eq. (4.1)]. Table 1 presents exact values of the total error rate when $\gamma = -2$ dB. According to these results, the total error rate is four and six times less for diversity receivers in comparison to non-diversity receivers at $\gamma_{th} = 5$ dB, as well as two and ten times less for diversity receivers at $\gamma_{th} = 15$ dB for the pLS and the pLC techniques, respectively. Moreover, the pLS diversity scheme shows better performance than the pLC technique. A lower threshold guarantees a high P_D at the cost of a low P_F. Hence, the total error rate is higher for $\gamma_{th} = 15$ dB. In Fig. 4, we present ROC curves over AWGN channels given $p = 10, \kappa = 0.5$ for hardware impaired system and $N = 10$. By varying $\gamma = -20; -5; 5; 10$ dB we plot ROC curves for ideal and non-ideal hardware models. At very low γ values, there is no effect of hardware impairment on the ROC curve, since AWGN noise component power dominates over hardware impairment noises, which is proportional to γ. As expected, higher γ values result in better ROC performance.

TABLE 1. Total error rate for non-diversity and diversity receivers at $\gamma = -2$ dB.

Total Error Rate	γ_{th}=5 dB	γ_{th}=15 dB
No diversity, $\kappa = 0$	0.3	0.5350
No diversity, $\kappa = 0.4$	0.35	0.5411
pLS, $\kappa = 0$	0.05	0.05
pLS, $\kappa = 0.4$	0.0501	0.0502
pLC, $\kappa = 0$	0.0713	0.2405
pLC, $\kappa = 0.4$	0.0794	0.2755

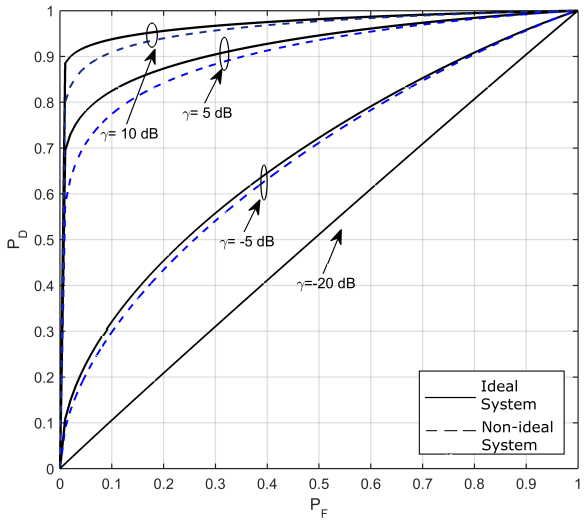

FIGURE 4. ROC curves at varying γ values over AWGN channel.

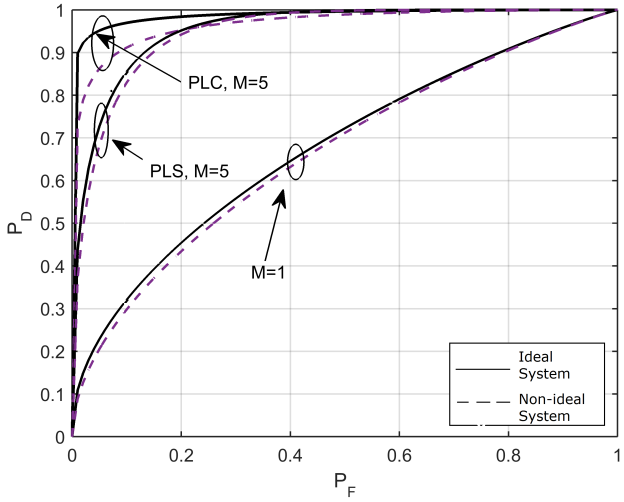

FIGURE 5. ROC curves for diversity and non-diversity receivers over Rayleigh fading channels.

The performance of the IED is shown using the ROC curves for Rayleigh fading scenario as shown in Fig. 5 using following system settings: $\bar{\gamma} = 5$ dB, $N = 10, p = 10$, $\kappa = 0.4$, $m = 1$, and number of diversity branches $M = 5$. At the given scenario, the pLC diversity technique performs better than the pLS technique, however it suffers more from hardware impairments in comparison to the pLS diversity technique and non-diversity receiver.

The AUC performance analysis is used to quantify the detection ability of the detector. In Fig. 6, we show the average AUC versus $\bar{\gamma}$ for $p = 4$, $p = 6$, and $p = 10$ for different number of signal samples, $N = 5$; 10, at ideal ($\kappa = 0$) and non-ideal ($\kappa = 0.3$) system modes over AWGN channel. From Fig. 6, we can clearly notice that ideal detectors outperform hardware impaired ones. In addition, the higher order IEDs show better detection capability. For

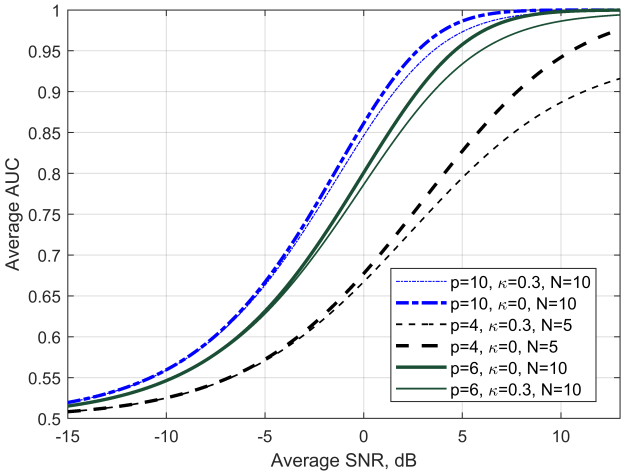

FIGURE 6. The average AUC versus average SNR for $p = 4$; 6; 10 over AWGN channel.

instance, at IED order $p = 10$, the AUC curve shows the highest performance, whereas when the IED order is $p = 4$ the AUC curve shows the lowest performance. Detection capability of the IED increases with the order p of the detector and number of signal samples.

VIII. CONCLUSION

In this paper, we have shown that transceiver hardware impairment noises degrade PU detection probability, and increase the total error rate. Moreover, the negative effect of distortion noises were more severe at non-diversity receivers. The IED performance under transceiver imperfections has not been studied in an open technical literature yet. Hence, we provided an insight on the performance of the IED under transceiver hardware constraints. A novel method was introduced on evaluating the IED using α-μ distribution. Closed-form expressions for evaluating the detection and the false alarm probabilities were evaluated for AWGN and Nakagami-m fading channels considering ideal and non-ideal system configurations. Asymptotic analysis of the average detection probability at very low γ values has been studied as well. Our numerical results proved that the pLC and the pLS diversity techniques were able to significantly improve detector performance. Moreover, the non-diversity receiver case was the most impaired by imperfection noises, whereas the pLS scheme was the least affected by hardware impairment noises. The total error rate performance was improved when the number of receive antennas were increased from 1 to 20, at the same time hardware impairment effects were reduced.

APPENDIX A
DERIVATION OF THE MOMENTS FOR WEIBULL SUMMANDS

Closed-form expressions for evaluating the exact moments of $\alpha - \mu$ distribution $\mathbb{E}[\Lambda]$, $\mathbb{E}[\Lambda^2]$, and $\mathbb{E}[\Lambda^4]$ will be discussed in this section. By using (13) and (14), $\mathbb{E}[\Lambda]$ can be calculated

as

$$\begin{aligned}
&\mathbb{E}[\Lambda] \\
&= \binom{1}{0}\binom{0}{0}\cdots\binom{0}{0}\mathbb{E}[\Lambda_1^1]\mathbb{E}[\Lambda_2^0]...\mathbb{E}[\Lambda_N^0] \\
&\quad+\binom{1}{1}\binom{1}{0}\cdots\binom{0}{0}\mathbb{E}[\Lambda_1^0]\mathbb{E}[\Lambda_2^1]...\mathbb{E}[\Lambda_N^0] \\
&\quad+\binom{1}{1}\binom{1}{1}\binom{1}{0}\cdots\binom{0}{0}\mathbb{E}[\Lambda_1^0]\mathbb{E}[\Lambda_2^0]\mathbb{E}[\Lambda_3^0]...\mathbb{E}[\Lambda_N^0] \\
&\quad+\binom{1}{1}\binom{1}{1}\cdots\binom{1}{1}\mathbb{E}[\Lambda_1^0]\mathbb{E}[\Lambda_2^0]...\mathbb{E}[\Lambda_N^1] \\
&= \mathbb{E}[\Lambda_1^1]+\mathbb{E}[\Lambda_2^1]+\mathbb{E}[\Lambda_3^1]+\cdots\mathbb{E}[\Lambda_N^1] \\
&= \Phi^{\frac{1}{\beta}}\Gamma(1+\frac{1}{\beta})+\Phi^{\frac{1}{\beta}}\Gamma(1+\frac{1}{\beta})+\cdots+\Phi^{\frac{1}{\beta}}\Gamma(1+\frac{1}{\beta}) \\
&= N\Phi^{\frac{1}{\beta}}\Gamma\Big(1+\frac{1}{\beta}\Big). \qquad (38)
\end{aligned}$$

Derivation steps for the $\alpha-\mu$ moment of order two can be represented as

$$\begin{aligned}
&\mathbb{E}[\Lambda^2] \\
&= \sum_{n_1=0}^{2}\sum_{n_2=0}^{n_1}\cdots\sum_{n_{N-1}=0}^{n_{N-2}}\binom{2}{n_1}\binom{n_1}{n_2}\cdots\binom{n_{N-2}}{n_{N-1}} \\
&\quad\times\mathbb{E}[\Lambda_1^{2-n_1}]\mathbb{E}[\Lambda_2^{n_1-n_2}]\cdots\mathbb{E}[\Lambda_N^{n_{N-1}}] \\
&\quad\binom{2}{0}\binom{0}{0}\cdots\binom{0}{0}\binom{0}{0}\mathbb{E}[\Lambda_1^2]\mathbb{E}[\Lambda_2^0]...\mathbb{E}[\Lambda_{N-1}^0]\mathbb{E}[\Lambda_N^0] \\
&\quad+\binom{2}{1}\binom{1}{0}\cdots\binom{0}{0}\binom{0}{0}\mathbb{E}[\Lambda_1^1]\mathbb{E}[\Lambda_2^1]...\mathbb{E}[\Lambda_{N-1}^0]\mathbb{E}[\Lambda_N^1] \\
&\quad\cdots \\
&\quad+\binom{2}{2}\binom{2}{2}\cdots\binom{2}{2}\binom{2}{1}\mathbb{E}[\Lambda_1^0]\mathbb{E}[\Lambda_2^0]...\mathbb{E}[\Lambda_{N-1}^1]\mathbb{E}[\Lambda_N^1] \\
&\quad+\binom{2}{2}\binom{2}{2}\cdots\binom{2}{2}\binom{2}{2}\mathbb{E}[\Lambda_1^0]\mathbb{E}[\Lambda_2^0]...\mathbb{E}[\Lambda_{N-1}^0]\mathbb{E}[\Lambda_N^2] \\
&= \mathbb{E}[\Lambda_1^1]+2\mathbb{E}[\Lambda_1^1]\mathbb{E}[\Lambda_2^1]+2\mathbb{E}[\Lambda_1^1]\mathbb{E}[\Lambda_3^1]+...+2\mathbb{E}[\Lambda_1^1] \\
&\quad\times\mathbb{E}[\Lambda_{N-1}^1]+2\mathbb{E}[\Lambda_1^1]\mathbb{E}[\Lambda_N^1]+\mathbb{E}[\Lambda_2^2]+2\mathbb{E}[\Lambda_2^1]\mathbb{E}[\Lambda_3^1] \\
&\quad+...2\mathbb{E}[\Lambda_2^1]\mathbb{E}[\Lambda_N^1]+\mathbb{E}[\Lambda_3^2]+2\mathbb{E}[\Lambda_3^1]\mathbb{E}[\Lambda_N^1] \\
&\quad+...+\mathbb{E}[\Lambda_{N-1}^2]+2\mathbb{E}[\Lambda_{N-1}^1]E[\Lambda_N^1]+\mathbb{E}[\Lambda_N^2]. \qquad (39)
\end{aligned}$$

By further expanding $\mathbb{E}[\Lambda_i^n]$ terms, we get closed-form solution for $\mathbb{E}[\Lambda^2]$ given in (16). Similarly, we present derivation of $\mathbb{E}[\Lambda^4]$ for $n=4$ by referring to (13)

$$\begin{aligned}
&\mathbb{E}[\Lambda^4] \\
&= \binom{4}{0}\binom{0}{0}\cdots\binom{0}{0}\binom{0}{0}\mathbb{E}[\Lambda_1^4]\mathbb{E}[\Lambda_2^0]...\mathbb{E}[\Lambda_{N-1}^0] \\
&\quad\times\mathbb{E}[\Lambda_N^0]+\binom{4}{1}\binom{1}{1}\cdots\binom{0}{0}\binom{0}{0}\mathbb{E}[\Lambda_1^3]\mathbb{E}[\Lambda_2^1]... \\
&\quad\times\mathbb{E}[\Lambda_{N-1}^0]\times\mathbb{E}[\Lambda_N^0]\cdots \\
&\quad+\binom{4}{1}\binom{1}{1}\cdots\binom{1}{1}\binom{1}{1}\mathbb{E}[\Lambda_1^3]\mathbb{E}[\Lambda_2^0]...\mathbb{E}[\Lambda_{N-1}^0] \\
&\quad\times\mathbb{E}[\Lambda_N^0]... \\
&\quad\cdots \\
&\quad+\binom{4}{4}\binom{4}{4}\cdots\binom{4}{4}\binom{4}{4}\mathbb{E}[\Lambda_1^0]\mathbb{E}[\Lambda_2^0]...\mathbb{E}[\Lambda_{N-1}^0]\mathbb{E}[\Lambda_N^4] \\
&= \mathbb{E}[\Lambda_1^4]+4\mathbb{E}[\Lambda_1^3]\mathbb{E}[\Lambda_2^1]+4\mathbb{E}[\Lambda_1^3]\mathbb{E}[\Lambda_3^1]+...+4\mathbb{E}[\Lambda_1^3] \\
&\quad\times\mathbb{E}[\Lambda_N^1]+\mathbb{E}[\Lambda_2^1]\mathbb{E}[\Lambda_2^2]+12\mathbb{E}[\Lambda_1^2]\mathbb{E}[\Lambda_2^1]\mathbb{E}[\Lambda_3^1]+... \\
&\quad+12\mathbb{E}[\Lambda_1^2]\mathbb{E}[\Lambda_2^1]\mathbb{E}[\Lambda_N^1]+6\mathbb{E}[\Lambda_1^2]\mathbb{E}[\Lambda_3^2]+12\mathbb{E}[\Lambda_1^2] \\
&\quad\times\mathbb{E}[\Lambda_3^1]\mathbb{E}[\Lambda_4^1]...+12\mathbb{E}[\Lambda_1^2]\mathbb{E}[\Lambda_3^1]\mathbb{E}[\Lambda_N^1]... \\
&\quad\cdots \\
&\quad+4\mathbb{E}[\Lambda_2^1]\mathbb{E}[\Lambda_N^3]+\mathbb{E}[\Lambda_3^4]+...+\mathbb{E}[\Lambda_N^4]. \qquad (40)
\end{aligned}$$

We partially represent Weibull summand terms of $E[\Lambda^4]$ in (40). After some algebraic manipulations and expanding Weibull moment terms we get the final closed-form expression for the fourth order $\alpha-\mu$ distribution given in (17).

APPENDIX B
CALCULATION OF THE AUC OVER AWGN CHANNEL

Derivation of the AUC over AWGN channel in (24) is given by

$$A(\gamma)=\int_0^1 P_D(P_F)dP_F. \qquad (41)$$

P_F is a function of γ_{th}, therefore the variable of integration is changed, which results in

$$A(\gamma)=\int_{\infty}^{0} P_D(\gamma,\gamma_{th})\frac{dP_F(\gamma_{th})}{\gamma_{th}}d\gamma_{th}, \qquad (42)$$

where limits of integration are found as $\gamma_{th}=\infty\rightarrow\Gamma(\mu_0,\infty)=0\rightarrow P_F(\gamma_{th})=0$ and $\gamma_{th}=0\rightarrow\Gamma(\mu_0,0)=\Gamma(\mu_0)\rightarrow P_F(\gamma_{th})=1$. We expand the $\frac{dP_F(\gamma_{th})}{d\gamma_{th}}$ term as

$$\begin{aligned}
\frac{dP_F(\gamma_{th})}{d\gamma_{th}} &= \frac{1}{\Gamma(\mu_0)}\frac{d}{d\gamma_{th}}(\Gamma(\mu_0,\psi_0)) \\
&= \frac{1}{\Gamma(\mu_0)}\frac{d}{d\gamma_{th}}\int_{\psi_0}^{\infty}t^{\mu_0-1}e^{-t}dt \qquad (43)
\end{aligned}$$

We evaluate Ω_0 and Ω_1 by using (18). Next, with the aid of $\psi_0=\frac{\mu_0\gamma_{th}^{\alpha_0}}{\Omega_0}$ and the Leibniz rule, we get

$$\begin{aligned}
&\frac{d}{d\gamma_{th}}\int_{\frac{\mu_0\gamma_{th}^{\alpha_0}}{\Omega_0}}^{\infty}t^{\mu_0-1}e^{-t}dt \\
&\quad= t^{\mu_0-1}e^{-t}\Big|_{t=\infty}-t^{\mu_0-1}e^{-t}\Big|_{t=\frac{\mu_0\gamma_{th}^{\alpha_0}}{\Omega_0}}\frac{\alpha_0\mu_0\gamma_{th}^{\alpha_0-1}}{\Omega_0} \\
&\quad+\int_{\frac{\mu_0\gamma_{th}^{\alpha_0}}{\Omega_0}}^{\infty}\frac{d}{d\gamma_{th}}(t^{\mu_0-1}e^{-t})dt \qquad (44)
\end{aligned}$$

Now, by substituting (20) and (44) into (42) and using [30, eq. (6.455)], we get

$$\begin{aligned}
A(\gamma)=\int_0^{\infty}\frac{\Gamma(\mu_1,\frac{\mu_1\gamma_{th}^{\alpha_1}}{\Omega_1})}{\Gamma(\mu_1)\Gamma(\mu_0)}\frac{\alpha_0}{\gamma_{th}}\Big(\frac{\mu_0\gamma_{th}^{\alpha_0}}{\Omega_0}\Big)^{\mu_0}\exp\Big(-\frac{\mu_0\gamma_{th}^{\alpha_0}}{\Omega_0}\Big) \\
\times d\gamma_{th}, \qquad (45)
\end{aligned}$$

where limits of integration where switched by minus sign. The following substitutions $\alpha_1=\alpha_0=\alpha$ and the change

of variables $\gamma_{th}^{\alpha} = s$, $d\gamma_{th} = \frac{1}{\alpha}s^{(\frac{1}{\alpha}-1)}ds$, as well as Ω_1 and Ω_0 parameters expansions in (45) lead to the final expression given in (24).

APPENDIX C
DERIVATION OF $\bar{P}_{DNak}^{id}$ OVER NAKAGAMI-m FADING CHANNELS

Derivation of the average detection probability $\bar{P}_{DNak}^{id}$ over Nakagami-m fading for ideal system model is shown as

$$\begin{aligned}\bar{P}_{DNak}^{id} &= \epsilon \int_0^{\infty} \gamma^{m-1} e^{-\frac{\gamma m}{\bar{\gamma}}} \times \left(\Gamma(\mu_1) - \sum_{n=0}^{\infty} \frac{(-1)^n \psi_1^{\mu_1+n}}{n!(\mu_1+n)(\gamma+1)^{\frac{\alpha_1(\mu_1+n)}{\beta}}}\right) d\gamma \\ &= \underbrace{\epsilon\Gamma(\mu_1)\int_0^{\infty} \gamma^{m-1} e^{-\frac{\gamma m}{\bar{\gamma}}} d\gamma}_{C1} \\ &\quad \underbrace{-\epsilon \sum_{n=0}^{\infty} \frac{(-1)^n \psi_1^{\mu_1+n}}{n!(\mu_1+n)} \int_0^{\infty} \gamma^{m-1} e^{-\frac{\gamma m}{\bar{\gamma}}} \left(\frac{1}{\gamma+1}\right)^{\frac{\alpha_1(\mu_1+n)}{\beta}} d\gamma}_{C2}. \end{aligned} \tag{46}$$

By using (28), integral of the part $C1$ is found as

$$C1 = \epsilon\Gamma(\mu_1)\Gamma(m)\left(\frac{m}{\bar{\gamma}}\right)^{-m} = 1, \tag{47}$$

where $m > 0$ and $\frac{m}{\bar{\gamma}} > 0$. By making use of the power of binomials in [30, eq. (1.110)], we represent power of the ratio as the summation terms given as

$$\left(\frac{1}{\gamma+1}\right)^s = \left(1 - \frac{\gamma}{\gamma+1}\right)^s = \sum_{j=0}^{\infty} \binom{s}{j} (-1)^j \left(\frac{\gamma}{\gamma+1}\right)^j, \tag{48}$$

where $\left(1 - \frac{\gamma}{\gamma+1}\right) < 1$ and $s = \frac{\alpha_1(\mu_1+n)}{\beta}$. Next, the integral of the $C2$ part in (46) is evaluated as

$$C2 = \epsilon \sum_{n=0}^{\infty}\sum_{j=0}^{\infty} \frac{(-1)^n(-1)^j}{n!(\mu_1+n)} \psi_1^{\mu_1+n} \binom{s}{j} \times \underbrace{\int_0^{\infty} \gamma^{m+j-1} e^{-\frac{\gamma m}{\bar{\gamma}}} \frac{1}{(1+\gamma)^j} d\gamma}_{C3}, \tag{49}$$

where we evaluate $C3$ as

$$\begin{aligned} C3 &= \int_0^{\infty} \gamma^{m+j-1} e^{-\frac{\gamma m}{\bar{\gamma}}} \frac{1}{(1+\gamma)^j} d\gamma \\ &= \int_0^{\infty} \sum_{k=0}^{m+j-1} \binom{m+j-1}{k} (1+\gamma)^{m+j-1-k} (-1)^k \times e^{-\frac{\gamma m}{\bar{\gamma}}} \frac{1}{(\gamma+1)^j} d\gamma \\ &= \sum_{k=0}^{m+j-1} \binom{m+j-1}{k} (-1)^k \underbrace{\int_0^{\infty} (\gamma+1)^{m-1-k} e^{-\frac{\gamma m}{\bar{\gamma}}} d\gamma}_{C4}. \end{aligned} \tag{54}$$

Now by using the change of variables and limits of the integral in (54) as $\gamma + 1 = s$ and $\gamma = 0 \Rightarrow s = 1$ and $\gamma = \infty \Rightarrow s = \infty$, we get the following integral

$$C4 = \int_0^{\infty} \left(s\frac{m}{\bar{\gamma}}\right)^{m-1-k} e^{-\frac{sm}{\bar{\gamma}}} d(s\frac{m}{\bar{\gamma}})(\frac{m}{\bar{\gamma}})^{k-m}. \tag{55}$$

Next, we take another turn of variable and limit change of the integral in (55) as $\frac{sm}{\bar{\gamma}} = z$, $s = 1 \Rightarrow z = \frac{m}{\bar{\gamma}}$ and $s = \infty \Rightarrow z = \infty$. Hence, we get the following expression

$$\begin{aligned} C4 &= \left(\frac{m}{\bar{\gamma}}\right)^{k-m} \int_{\frac{m}{\bar{\gamma}}}^{\infty} z^{m-1-k} e^{-z} dz \\ &= \left(\frac{m}{\bar{\gamma}}\right)^{k-m} \Gamma\left(m-k, \frac{m}{\bar{\gamma}}\right). \end{aligned} \tag{56}$$

Final solution for the P_{DNak}^{id} is found by placing $C3$ into $C2$ and displayed in (27).

APPENDIX D
DERIVATION OF $\bar{P}_{DNak}^{hi}$ AT NON-IDEAL SYSTEM MODEL

Calculation of the average detection probability for ideal system model over Nakagami-m fading channel was presented in Appendix C. Similar approach is used to derive the average detection probability over Nakagami-m fading channel for hardware impaired system model. Instead of γ in (46) we replace SNDR, γ_{hi}, given in (2) and calculate $\bar{P}_{DNak}^{hi}$ (53), as shown at the top of next page.

where the integral of $D1$ is shown in (47). By using [30, eq. (1.110)], we expand and calculate the $D3$ part as

$$\begin{aligned} D3 &= \left(\frac{1}{\frac{\gamma}{k^2\gamma+1}+1}\right)^{\frac{\alpha_1(\mu_1+n)}{\beta}} = \left(1 - \frac{\gamma}{\gamma+\gamma\kappa^2+1}\right)^{\frac{\alpha_1(\mu_1+n)}{\beta}} \\ &= \sum_{j=0}^{\infty} \binom{\frac{\alpha_1(\mu_1+n)}{\beta}}{j} \left(-\frac{\gamma}{\gamma+\gamma\kappa^2+1}\right)^j. \end{aligned} \tag{54}$$

Hence, the integral of the $D2$ is found as follows

$$D2 = \epsilon \sum_{n=0}^{\infty}\sum_{j=0}^{\infty} \frac{(-1)^n (-1)^j \psi_1^{\mu_1+n}}{n!(\mu_1+n)} \binom{\frac{2}{\beta}(\mu_1+n)}{j} \times \underbrace{\int_0^{\infty} \underbrace{\gamma^{m+j-1}}_{D5} e^{-\frac{m\gamma}{\bar{\gamma}}} \frac{1}{\left(\gamma\left(1+k^2\right)+1\right)^j} d\gamma}_{D4}. \tag{55}$$

Next, we evaluate the integral given in (55) with the following conversion of the $D5 = \gamma^{m+j-1} = \frac{(\gamma\tau)^{m+j-1}}{\tau^{m+j-1}} = \frac{(\gamma\tau+1-1)^{m+j-1}}{\tau^{m+j-1}}$ and $\tau = 1 + \kappa^2$. By using the power of

$$\bar{P}_{DNak}^{\text{hi}} = \epsilon \int_0^\infty \gamma^{m-1} e^{-\frac{\gamma m}{\bar{\gamma}}} \times \Big(\Gamma(\mu_1) - \sum_{n=0}^{\infty} \frac{(-1)^n \psi_1^{\mu_1+n}}{n!(\mu_1+n)(\frac{\gamma}{k^2\gamma+1}+1)^{\frac{\alpha_1(\mu_1+n)}{\beta}}}\Big) d\gamma$$

$$= \underbrace{\epsilon\Gamma(\mu_1) \int_0^\infty \gamma^{m-1} e^{-\frac{\gamma m}{\bar{\gamma}}} d\gamma}_{\text{D1}} - \underbrace{\epsilon \sum_{n=0}^{\infty} \frac{(-1)^n \psi_1^{\mu_1+n}}{n!(\mu_1+n)} \int_0^\infty \gamma^{m-1} e^{-\frac{\gamma m}{\bar{\gamma}}} \underbrace{\Big(\frac{1}{\frac{\gamma}{k^2\gamma+1}+1}\Big)^{\frac{\alpha_1(\mu_1+n)}{\beta}}}_{D3} d\gamma}_{D2}, \quad (53)$$

binomials, $D5$ is expressed as

$$D5 = \tau^{-j-m+1} \sum_{t=0}^{j+m-1} (-1)^t \binom{j+m-1}{t} (\tau\gamma+1)^{m+j-1-t}. \quad (56)$$

Hence, the integral of the $D4$ can be evaluated as

$$\begin{aligned} D4 &= \int_0^\infty \exp\Big(-\frac{m(\gamma\tau+1)}{\bar{\gamma}\tau}\Big) \exp\Big(\frac{m}{\bar{\gamma}\tau}\Big) \frac{1}{(\gamma\tau+1)^j} \\ &\quad \times \frac{1}{\tau^{j+m-1}} \sum_{t=0}^{j+m-1} (-1)^t \binom{j+m-1}{t} \Big(\frac{m}{\tau\bar{\gamma}}\Big)^{t-m} \\ &= \frac{\exp\left(\frac{m}{\bar{\gamma}\tau}\right)}{\tau^{m+j-1}} \sum_{t=0}^{j+m-1} \binom{j+m-1}{t} (-1)^t \\ &\quad \times \int_0^\infty \underbrace{\exp\Big(-\frac{m(\gamma\tau+1)}{\bar{\gamma}\tau}\Big)}_{\text{D6}} (\gamma\tau+1)^{m-t-1} d\gamma. \quad (57) \end{aligned}$$

In order to solve the above integral in (57), we used the variable and limit change as $s = \gamma\tau + 1$, $\gamma = 0 \Rightarrow s = 1$ and $\gamma = \infty \Rightarrow s = \infty$ and present the integral as

$$D6 = \frac{1}{\tau} \int_1^\infty \Big(\frac{ms}{\bar{\gamma}\tau}\Big)^{m-t-1} \exp\Big(-\frac{ms}{\bar{\gamma}\tau}\Big) \Big(\frac{m}{\bar{\gamma}\tau}\Big)^{t-m} d\Big(\frac{ms}{\bar{\gamma}\tau}\Big). \quad (58)$$

Next, we change the integral variables of the (58) as $z = \frac{ms}{\bar{\gamma}\tau}$, and exchange the limits as $s = 1 \Rightarrow z = \frac{m}{\bar{\gamma}\tau}$ and $s = \infty \Rightarrow z = \infty$, and finally solve the integral as

$$\begin{aligned} D6 &= \frac{1}{\tau} \int_{\frac{m}{\bar{\gamma}\tau}}^\infty z^{m-t-1} e^{-z} dz \Big(\frac{m}{\bar{\gamma}\tau}\Big)^{t-m} \\ &= \frac{1}{\tau} \Gamma\Big(m-t, \frac{m}{\tau\bar{\gamma}}\Big) \Big(\frac{m}{\tau\bar{\gamma}}\Big)^{t-m}. \quad (59) \end{aligned}$$

Now, by placing the $D4$ and the $D5$ parts into the $D2$, we get the final expression that represents $\bar{P}_{DNak}^{\text{hi}}$ given in (29).

REFERENCES

[1] F. F. Digham, M.-S. Alouini, and M. K. Simon, "On the energy detection of unknown signals over fading channels," *IEEE Trans. Commun.*, vol. 55, no. 1, pp. 21–24, Jan. 2007.

[2] Y. Chen, "Improved energy detector for random signals in Gaussian noise," *IEEE Trans. Wireless Commun.*, vol. 9, no. 2, pp. 558–563, Feb. 2010.

[3] A. Singh, M. R. Bhatnagar, and R. K. Mallik, "Performance of an improved energy detector in multihop cognitive radio networks," *IEEE Trans. Veh. Technol.*, vol. 65, no. 2, pp. 732–743, Feb. 2016.

[4] L. Gahane, P. K. Sharma, N. Varshney, T. A. Tsiftsis, and P. Kumar, "An improved energy detector for mobile cognitive users over generalized fading channels," *IEEE Trans. Commun.*, vol. 66, no. 2, pp. 534–545, Feb. 2017.

[5] S. Nallagonda, S. D. Roy, S. Kundu, G. Ferrari, and R. Raheli, "Censoring-based cooperative spectrum sensing with improved energy detectors and multiple antennas in fading channels," *IEEE Trans. Aerosp. Electron. Syst.*, vol. 54, no. 2, pp. 537–553, Apr. 2018.

[6] S. K. Sharma, T. E. Bogale, S. Chatzinotas, B. Ottersten, L. B. Le, and X. Wang, "Cognitive radio techniques under practical imperfections: A survey," *IEEE Commun. Surveys Tuts.*, vol. 17, no. 4, pp. 1858–1884, 4th Quart., 2015.

[7] L. Gahane and P. K. Sharma, "Performance of improved energy detector with cognitive radio mobility and imperfect channel state information," *IET Commun.*, vol. 11, no. 12, pp. 1857–1863, 2017.

[8] M. Ranjeeth, S. Behera, S. Nallagonda, and S. Anuradha, "Optimization of cooperative spectrum sensing based on improved energy detector with selection diversity in AWGN and Rayleigh fading," in *Proc. Int. Conf. Elect., Electron., Optim. Techn. (ICEEOT)*, Mar. 2016, pp. 2402–2406.

[9] L. Safatly, A. El-Hajj, and K. Y. Kabalan, "Blind and robust spectrum sensing based on RF impairments mitigation for cognitive radio receivers," in *Proc. Int. Conf. High Perform. Comput. Simulation (HPCS)*, Jul. 2014, pp. 820–824.

[10] A.-A. A. Boulogeorgos, N. D. Chatzidiamantis, and G. K. Karagiannidis, "Energy detection spectrum sensing under RF imperfections," *IEEE Trans. Commun.*, vol. 64, no. 7, pp. 2754–2766, Jul. 2016.

[11] O. Semiari, B. Maham, and C. Yuen, "On the effect of I/Q imbalance on energy detection and a novel four-level hypothesis spectrum sensing," *IEEE Trans. Veh. Technol.*, vol. 63, no. 8, pp. 4136–4141, Oct. 2014.

[12] E. Y. Imana, T. Yang, and J. H. Reed, "Suppressing the effects of aliasing and IQ imbalance on multiband spectrum sensing," *IEEE Trans. Veh. Technol.*, vol. 66, no. 2, pp. 1074–1086, Feb. 2017.

[13] A. Mehrabian and A. Zaimbashi, "Spectrum sensing in SIMO cognitive radios under primary user transmitter IQ imbalance," *IEEE Syst. J.*, to be published, doi: 10.1109/JSYST.2018.2850960.

[14] A. Gokceoglu, Y. Zou, M. Valkama, and P. C. Sofotasios, "Multi-channel energy detection under phase noise: Analysis and mitigation," *Mobile Netw. Appl.*, vol. 19, no. 4, pp. 473–486, Aug. 2014.

[15] A. Gokceoglu, S. Dikmese, M. Valkama, and M. Renfors, "Energy detection under IQ imbalance with single- and multi-channel direct-conversion receiver: Analysis and mitigation," *IEEE J. Sel. Areas Commun.*, vol. 32, no. 3, pp. 411–424, Mar. 2014.

[16] A.-A. A. Boulogeorgos, H. A. B. Salameh, and G. K. Karagiannidis, "Spectrum sensing in full-duplex cognitive radio networks under hardware imperfections," *IEEE Trans. Veh. Technol.*, vol. 66, no. 3, pp. 2072–2084, Mar. 2017.

[17] E. Bjornson, M. Matthaiou, and M. Debbah, "A new look at dual-hop relaying: Performance limits with hardware impairments," *IEEE Trans. Commun.*, vol. 61, no. 11, pp. 4512–4525, Nov. 2013.

[18] D. K. Nguyen, T. T. Lam, and H. Ochi, "Performance analysis: DF cognitive network with transceiver imperfections," in *Proc. 48th Asilomar Conf. Signals, Syst. Comput.*, Nov. 2014, pp. 1604–1608.

[19] D. K. Nguyen and H. Ochi, "Transceiver impairments in DF/AF dual-hop cognitive relay networks: Outage performance and throughput analysis," in *Proc. IEEE 81st Veh. Technol. Conf.*, Glasgow, U.K., May 2015, pp. 1–5.

[20] H. Huang, Z. Li, B. Ai, G. Wang, and M. S. Obaidat, "Impact of hardware impairment on spectrum underlay cognitive multiple relays network," in *Proc. IEEE Int. Conf. Commun. (ICC)*, May 2016, pp. 1–6.
[21] P. K. Sharma and P. K. Upadhyay, "Cognitive relaying with transceiver hardware impairments under interference constraints," *IEEE Commun. Lett.*, vol. 20, no. 4, pp. 820–823, Apr. 2016.
[22] A. K. Mishra, D. Mallick, and P. Singh, "Combined effect of RF impairment and CEE on the performance of dual-hop fixed-gain AF relaying," *IEEE Commun. Lett.*, vol. 20, no. 9, pp. 1725–1728, Sep. 2016.
[23] T. Schenk, *RF Imperfections in High-rate Wireless Systems: Impact and Digital Compensation*. Dordrecht, The Netherlands: Springer, 2008.
[24] B. E. Priyanto, T. B. Sorensen, O. K. Jensen, T. Larsen, T. Kolding, and P. Mogensen, "Assessing and modeling the effect of RF impairments on UTRA LTE uplink performance," in *Proc. IEEE 66th Veh. Technol. Conf.*, Sep. 2007, pp. 1213–1217.
[25] E. Balti, M. Guizani, B. Hamdaoui, and B. Khalfi, "Aggregate hardware impairments over mixed RF/FSO relaying systems with outdated CSI," *IEEE Trans. Commun.*, vol. 66, no. 3, pp. 1110–1123, Mar. 2018.
[26] X. Zhang, M. Matthaiou, M. Coldrey, and E. Björnson, "Impact of residual transmit RF impairments on training-based MIMO systems," *IEEE Trans. Commun.*, vol. 63, no. 8, pp. 2899–2911, Aug. 2015.
[27] H. Rinne, *The Weibull Distribution: A Handbook*, 1st ed. London, U.K.: Chapman & Hall, 2008.
[28] J. C. S. S. Filho and M. D. Yacoub, "Simple precise approximations to Weibull sums," *IEEE Commun. Lett.*, vol. 10, no. 8, pp. 614–616, Aug. 2006.
[29] M. D. Yacoub, "The $\alpha - \mu$ distribution: A physical fading model for the stacy distribution," *IEEE Trans. Veh. Technol.*, vol. 56, no. 1, pp. 27–34, Jan. 2007.
[30] I. Ryzhik and I. Gradshtein, *Table of Integrals, Series and Products*, 6th ed. San Diego, CA, USA: Academic, 2000.
[31] S. Atapattu, C. Tellambura, and H. Jiang, "Analysis of area under the ROC curve of energy detection," *IEEE Trans. Wireless Commun.*, vol. 9, no. 3, pp. 1216–1225, Mar. 2010.
[32] S. Atapattu, C. Tellambura, and H. Jiang, *Energy Detection for Spectrum Sensing in Cognitive Radio*. New York, NY, USA: Springer, 2014.
[33] S. Shanmugave and M. A. Bhagyaveni, *Cognitive Radio—An Enabler for Internet of Things*. Delft, The Netherlands: River Publishers, 2017.

LEILA TLEBALDIYEVA received the B.S. degree in communications engineering from Carleton University, Ottawa, ON, Canada, in 2010, and the M.Sc. degree in wireless and optical communications from University College London, London, U.K., in 2012. She is currently pursuing the Ph.D. degree with the Department of Electrical and Computer Engineering, Nazarbayev University, Astana, Kazakhstan. Her research interest includes spectrum sensing/sharing cognitive radio networks with hardware imperfections.

THEODOROS A. TSIFTSIS (S'02–M'04–SM'10) was born in Lamia, Greece, in 1970. He received the B.Sc. degree in physics from the Aristotle University of Thessaloniki, Greece, in 1993, the M.Sc. degree in digital systems engineering from Heriot-Watt University, Edinburgh, U.K., in 1995, the M.Sc. degree in decision sciences from the Athens University of Economics and Business, in 2000, and the Ph.D. degree in electrical engineering from the University of Patras, Greece, in 2006. He is currently a Full Professor with the School of Electrical and Information Engineering, Jinan University, Zhuhai, China. He has authored or co-authored over 150 technical papers in scientific journals and international conferences. His research interests include the broad areas of cooperative communications, cognitive radio, communication theory, wireless-powered communication systems, and optical wireless communication systems.

Dr. Tsiftsis acts as a Reviewer for several international journals and conferences. He has served as a Senior or Associate Editor in the Editorial Board of the IEEE TRANSACTIONS ON VEHICULAR TECHNOLOGY and the IEEE COMMUNICATIONS LETTERS. He is currently an Area Editor for Wireless Communications II of the IEEE TRANSACTIONS ON COMMUNICATIONS and an Associate Editor of the IEEE TRANSACTIONS ON MOBILE COMPUTING.

BEHROUZ MAHAM (S'07–M'10–SM'15) received the B.Sc. and M.Sc. degrees in electrical engineering from the University of Tehran, Tehran, Iran, in 2005 and 2007, respectively, and the Ph.D. degree from the University of Oslo, Oslo, Norway, in 2010. From 2008 to 2009, he was with the Department of Electrical Engineering, Stanford University, Stanford, CA, USA. He was a Faculty Member with the School of Electrical and Computer Engineering, University of Tehran, from 2011 to 2015. He is currently an Associate Professor with the School of Engineering, Nazarbayev University. He has more than 120 publications in major technical journals and conferences. His research interests include wireless communication and networking and nano-neural communication systems. He is a TWAS Affiliate.